Railway Engineering Science (2024) 32(2):229–243
https://doi.org/10.1007/s40534-023-00323-3

Torque effect on vibration behavior of high-speed train gearbox under internal and external excitations

Yue Zhou[1] · Xi Wang[1] · Hongbo Que[1,2] · Rubing Guo[2] · Xinhai Lin[2] · Siqin Jin[2] · Chengpan Wu[2] · Yu Hou[3]

Received: 23 May 2023 / Revised: 28 September 2023 / Accepted: 29 September 2023 / Published online: 14 November 2023

Abstract
The high-speed train transmission system, experiencing both the internal excitation originating from gear meshing and the external excitation originating from the wheel–rail interaction, exhibits complex dynamic behavior in the actual service environment. This paper focuses on the gearbox in the high-speed train to carry out the bench test, in which various operating conditions (torques and rotation speeds) were set up and the excitation condition covering both internal and external was created. Acceleration responses on multiple positions of the gearbox were acquired in the test and the vibration behavior of the gearbox was studied. Meanwhile, a stochastic excitation modal test was also carried out on the test bench under different torques, and the modal parameter of the gearbox was identified. Finally, the sweep frequency response of the gearbox under gear meshing excitation was analyzed through dynamic modeling. The results showed that the torque has an attenuating effect on the amplitude of gear meshing frequency on the gearbox, and the effect of external excitation on the gearbox vibration cannot be ignored, especially under the rated operating condition. It was also found that the torque affects the modal parameter of the gearbox significantly. The torque has a great effect on both the gear meshing stiffness and the bearing stiffness in the transmission system, which is the inherent reason for the changed modal characteristics observed in the modal test and affects the vibration behavior of the gearbox consequently.

Keywords High-speed train · Gearbox · Bench test · Vibration behavior · Modal identification

1 Introduction

The high-speed train gearbox transmission system is a gear–shaft–gearbox coupling system, which comprises a single-stage helical gear pair, an input shaft, a gearbox, and a wheelset, as shown in Fig. 1. The input torque that originates from the traction motor is transmitted to the wheelset through the gear pair to drive the train, and the gearbox will provide support to the input shaft. Due to the time-varying characteristic of the gear meshing stiffness (TVMS) and transmission errors (TEs), internal excitation exists in the transmission system [1–4], which will be transmitted to the gearbox through the gearbox bearing on the input shaft. Meanwhile, the interaction between the wheelset and the rail generates the external excitation inevitably [6, 7], which will also be transmitted to the gearbox through the gearbox bearing on the wheelset.

Both the internal excitation and external excitation are transmitted in the gearbox under the actual operating conditions, making the gearbox exhibits complex vibration behavior and have great effects on its fatigue reliability. Hu et al. [8] carried out a field test and discovered that wheel rail interaction can excite the modal vibration of the gearbox, which is the key factor of the fatigue crack development of the gearbox housing. A similar phenomenon was also found by Zhang et al. [9]. In order to ensure the safety and smooth operation of the high-speed train, it is of great significance to study the vibration behavior of a gearbox under internal and external excitation as well as its modal characteristics.

Considering the operational safety, it is difficult to carry out a field test of the high-speed train gearbox with a limited number of the sensors. Thus, the study on the vibration behavior of the gearbox usually adopts the way of simulation

✉ Xi Wang
wangxi@bjtu.edu.cn

1 School of Mechanical, Electronic and Control Engineering, Beijing Jiaotong University, Beijing 100044, China

2 CRRC Qishuyan Institute Co., Ltd., No. 258, Wuyi Road, Qishuyan, Changzhou 213011, China

3 Frontiers Science Center for Smart High-Speed Railway System, Beijing Jiaotong University, Beijing 100044, China

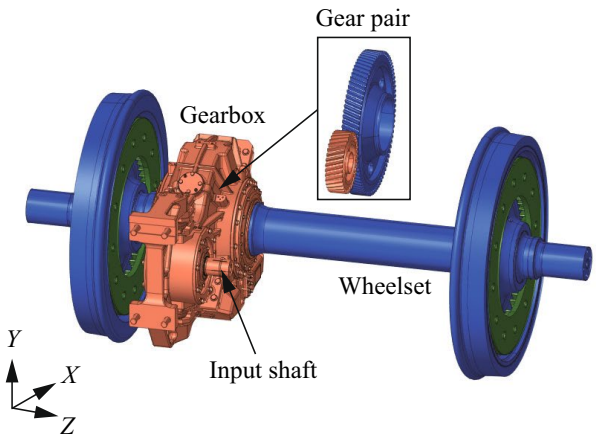

Fig. 1 High-speed train gearbox transmission system

and bench tests. Huang et al. [10, 11] established a gearbox vehicle railway dynamic model considering both internal and external excitations; they discovered that the effect of internal excitations on the gearbox vibration cannot be ignored when the vehicle is running at a high speed. As for the bench test of the high-speed train transmission system. Wang et al. [7] simulated the 20th-order polygonal excitation of the wheel on the test bench and studied the vibration behavior of the high-speed train gearbox under external excitation. Wei et al. [12] tested the vibration response of the high-speed train gearbox under different operating conditions and studied the vibration behavior of the gearbox under internal excitation. However, the simulation study of the high-speed train gearbox needs verification and an experimental study covering both internal and external excitations is lacking.

As for the modal characteristics of high-speed train gearboxes, experimental research usually adopts the way of operational modal analysis (OMA) and experimental modal analysis (EMA). Among them, OMA is more valuable because it can reflect the modal characteristics of a structure under real operational conditions. However, due to the periodic characteristic of internal excitations and the non-white noise characteristic of external excitations, the spurious mode needs to be distinguished from the identified modes in OMA when it is applied to a high-speed train gearbox, which usually requires advanced identification methods [13, 14]. In comparison, EMA outperforms in robustness and repeatability. Zhang et al. [16] conducted the stochastic excitation modal test on the high-speed train gearbox in the laboratory and acquired its modal parameters at the assembly condition, but the effect of torque is ignored in the test, which means that the operational modal characteristic of the gearbox cannot be accurately reflected.

In this study, both the internal and external excitations were considered in the bench test of a high-speed train gearbox to study its vibration behavior under various operating conditions. Meanwhile, a stochastic excitation modal test was also carried out on the test bench, and modal parameters of the gearbox were identified under different torque conditions. The sweep frequency response of the gearbox under gear meshing excitation is then analyzed to explain the phenomenon observed in the modal test through dynamic modeling. Consequently, the torque effect on both the vibration behavior and modal characteristics of the high-speed train gearbox is revealed.

1. Drive motor;
2. Universal joint;
3. Input shaft;
4. C-Shaped bracket;
5. Output shaft support bearing bench-1;
6. Vertical actuator-1;
7. Gearbox;
8. Output shaft;
9. Vertical actuator-2;
10. Output shaft support bearing bench-2.

Fig. 2 High-speed train gearbox transmission system test bench

2 Bench test set up

The experiment was conducted on a high-speed train gearbox transmission system test bench, as shown in Fig. 2. It contains two main sub-modules: a transmission module and an excitation module. The operating conditions of the transmission system, namely the torque and the rotation speed, can be controlled in a wide range through the transmission

module in the test bench. Meanwhile, the excitation module of the test bench provides vertical excitation through two electromagnetic actuators under two support-bearing benches of the output shaft.

2.1 Operating conditions

The torque and rotation speed of the test bench motor is related to the tracking curve of the high-speed train in the real operating scenario: Three input torques ranging from 500 to 1500 N·m and six vehicle speeds (V) ranging from 50 to 300 km/h are set up in the test. The rotation speed of the input shaft (ω_{is}) is related to the vehicle speed through Eq. (1), where z_p, z_g and D_w represent the pinon tooth number, gear tooth number, and the wheel diameter, respectively.

$$\omega_{is} = \frac{5z_g}{9D_w z_p} V. \tag{1}$$

Based on the relationship given above, the corresponding input shaft rotation speed of the vehicle speed (50–300 km/h) ranges from 750 to 4500 rpm. It should be mentioned that the combination of 4500 rpm and 500 N·m is the rated operating condition when the vehicle is running at the speed of 300 km/h. All of the working conditions in the bench test are listed in Table 1.

2.2 Generation of the railway vertical excitation signal

The external excitation signal of the actuator comes from the measured axle-box vertical acceleration response of the high-speed train running on the Wuhan–Guangzhou high-speed railway in China. The generation process of the railway vertical excitation signal is illustrated in Fig. 3. Figure 3a shows the vehicle speed curve as well as the axle-box vertical acceleration response. It can be seen that a total of seven inter-station periods exist in the vehicle speed curve and each inter-station period has one accelerating process and one decelerating process. Firstly, a 2-s time series is intercepted around the center of each speed condition in the accelerating and decelerating process, and the axle-box vertical acceleration is extracted based on those time series. A total of 14 segment signals of the axle-box vertical acceleration are extracted at each vehicle speed. Secondly, the power spectrum density (PSD) of those extracted signals is calculated and condensed into an averaged PSD spectrum, as shown in Fig. 3b. It can be seen that the vertical vibration of the axle box mainly occurs to the frequency range of 10 Hz–1 kHz, based on which, the upper and lower limits of the excitation frequency of the test bench electromagnetic actuator are determined. The one-way arrow in Fig. 3b represents the gear meshing frequency, which is filtered to prevent its repetitive influence on the gearbox. Thirdly, adding the random phase to the averaged PSD spectrum, the excitation signal is generated by inverse fast Fourier transform (IFFT), as shown in Fig. 3c. The acceleration response of the bearing bench (Fig. 2: 5) is compared with the excitation signal that is applied to the electromagnetic actuator (Fig. 2: 6) in the frequency domain at the rotation speed of 4500 rpm, as shown in Fig. 4. It can be seen that the two PSD spectrums almost overlap, which means that the excitation signal is well applied to the test bench.

Table 1 Operating conditions of the motor

Vehicle speed (km/h)	Rotation speed (rpm)	Input torque (N·m)		
		500	1000	1500
50	750	√	√	√
100	1500	√	√	√
150	2250	√	√	√
200	3000	√	√	√
250	3750	√	√	√
300	4500	√	√	√

The symbol '√'means that the operating condition was covered in the bench test

2.3 Acceleration sensor position

Acceleration responses in multiple positions of the gearbox were measured in the test, as shown in Fig. 5. It can be seen that a total of 12 three-directional piezoelectric acceleration sensors are equally distributed on both the wheel side (Fig. 5a) and motor side (Fig. 5b) of the gearbox. There are four acceleration sensors (A09–A12) installed at those four bearing benches on the gearbox. All of the acceleration sensors are sampled at the frequency of 10 kHz, which is sufficient to catch the gear meshing frequency under all rotation speeds.

3 Vibration behavior of the gearbox under different working conditions

The root mean square (RMS) of the acceleration values measured by sensors A09–A12 on the gearbox bearing bench is calculated under those operating conditions in Table 1, and the averaged RMS value is used to represent the overall vibration behavior of the gearbox. Figure 6 illustrates the averaged RMS under different input torques and rotation speeds in three directions (X, Y, Z). It can be seen that the averaged RMS values in directions X and Z present a similar variation trend with respect to the rotation speed, as they both reach the maximum value at the rotation speed of 2250 rpm and have a local minimum value at

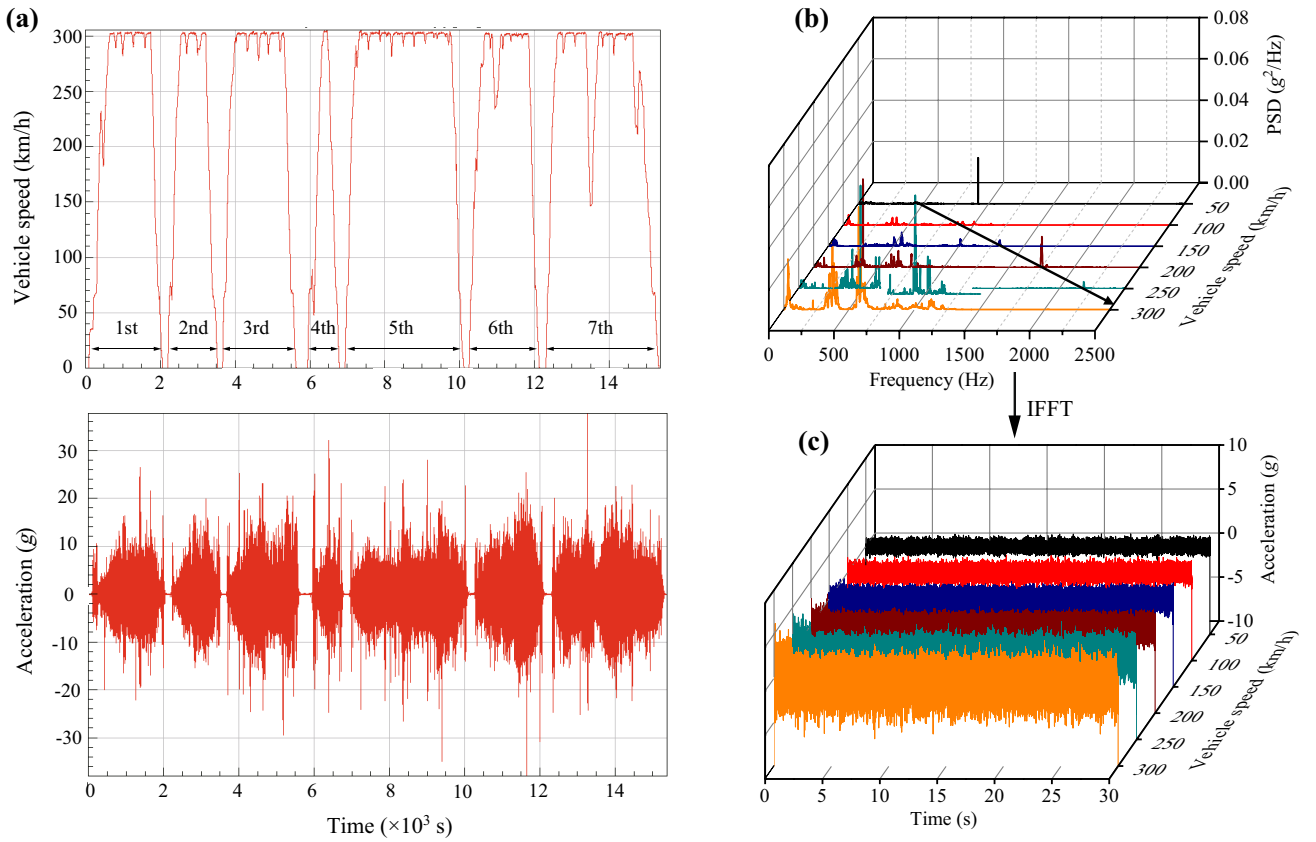

Fig. 3 Illustration of the railway vertical excitation generation process: **a** vehicle speed and axle-box vertical acceleration; **b** the calculated average PSD at target speeds; **c** acceleration excitation signals at different vehicle speeds

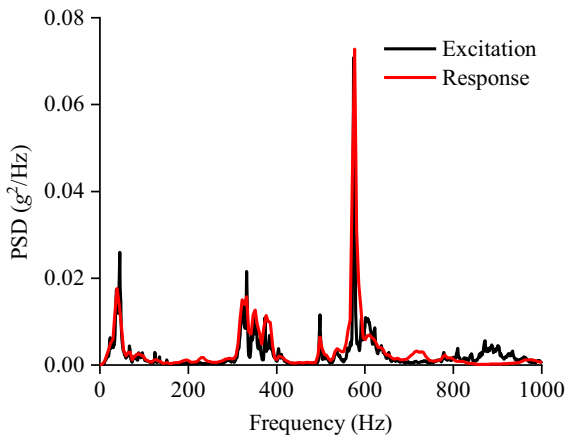

Fig. 4 Comparison between PSD spectrums of the acceleration response and the excitation signal at the rotation speed of 4500 rpm

the rotation speed of 3750 rpm. Meanwhile, the torque has a great effect on gearbox vibration in directions *X* and *Z*, as the averaged RMS decreases significantly at both 2250 and 3000 rpm when the input torque increases from 500 to 1500 N·m. However, the averaged RMS in direction *Y* varies differently with the rotation speed when compared with that in direction *X* and direction *Z*. It can be seen it reaches the maximum value at 3000 rpm under 500 N·m. When the torque increases from 500 and 1500 N·m, the rotation speed corresponding to the maximum averaged RMS value shifts from 3000 to 4500 rpm.

In order to reveal what led to the severe vibration of the gearbox at the rotation speeds of 2250 and 3000 rpm, the average acceleration–frequency spectrum of the bearing bench under different input torques in three directions are compared in Figs. 7 and 8, respectively. In Fig. 7, the labeled dash line represents the gear meshing frequency (f_m). Obviously, f_m dominates the average acceleration–frequency spectrum under all three input torques, which means that internal excitation is the key influencing factor of the gearbox vibration at the rotation speed of 2250 rpm. However, when the input torque varies from 500 to 1500 N·m, the acceleration amplitude at f_m decreases significantly in directions *X* and *Z*, but is nearly equivalent in direction *Y*. It just corresponds to the variation characteristic of the averaged RMS shown in Fig. 6. A similar phenomenon also exists at the rotation speed of 3000 rpm. In Fig. 8, f_m exhibits the primary status in the average acceleration–frequency spectrum

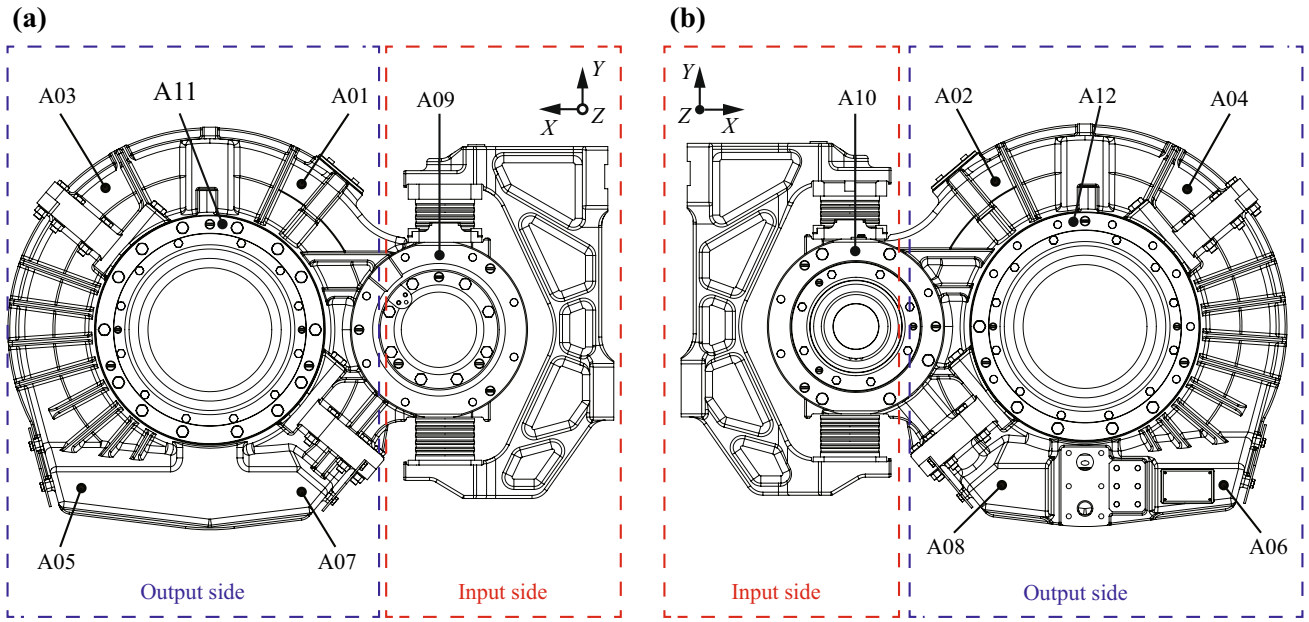

Fig. 5 Acceleration sensor positions on the gearbox: **a** wheel side; **b** motor side

and the amplitude of the vibration acceleration decreases with the increased input torque in all three directions. Additionally, the amplitude of two times the gear meshing frequency ($2f_m$) increases with the increased torque at both 2250 and 3000 rpm in the direction *Y*.

In summary, the vibration behavior of the gearbox is complex, as it differs a lot at different rotation speeds and in different directions. The torque affects the gearbox vibration greatly under the specified rotation speeds, namely 2250 and 3000 rpm. It is found that the gear meshing frequency (f_m) is the dominant vibration index in the gearbox acceleration response at the above two rotation speeds, and the increased torque will attenuate the amplitude of gear meshing frequency.

From Figs. 7 and 8, we know that the internal excitation (i.e., the gear meshing frequency f_m) is the key influencing factor of the gearbox vibration at the rotation speeds of 2250 and 3000 rpm, but what is the situation at the other rotation speeds? To make it clear, the torque condition of 500 N·m is selected to illustrate, under which the average acceleration–frequency spectrums at all six rotation speeds are compared in Fig. 9. The one-way arrow in Fig. 9 represents the gear meshing frequency (f_m) at different rotation speeds; its value and the corresponding acceleration are shown in the upper right corner in Fig. 9. It can be seen that the variation trend of the amplitude of acceleration at f_m is similar to that of the averaged RMS in Fig. 6 when the rotation speed varies from 750 to 3750 rpm, as they both increase first and then decrease with the rotation speed. However, the situation is quite different at the rotation speed of 4500 rpm. It can be seen the amplitude of acceleration at f_m in Fig. 9 is not as large as the averaged RMS in Fig. 6. Meanwhile, the amplitude of the vibration acceleration at frequencies below 1 kHz shows an increasing trend with the increased rotation speed, which means that the effect of external excitation (10 Hz–1 kHz) on the gearbox vibration becomes more and more significant when vehicle speed increases.

The average acceleration–frequency spectrum in three directions is zoomed-in in the frequency range of 0–1 kHz at the rotation speed of 4500 rpm and shown in Fig. 10a. It can be seen that the gearbox vibrations are mainly distributed within two frequency bands, namely 0–300 Hz and 500 Hz–1 kHz. In the frequency band of 0–300 Hz, the vibration frequencies labeled as f_p and $3f_p$ are identified to be the rotation speed and three times the rotation speed of the pinon, but the frequencies of 45 Hz and 70 Hz are unknown. In order to find out what these vibration frequencies represent, a short-time Fourier transform analysis is conducted on the response signal of the bearing bench in the direction *Y* during the accelerating state, and the average acceleration–time–frequency spectrum of the bearing bench is calculated, as shown in Fig. 10b. It can be seen that there is one vertical high brightness frequency band around 45 Hz and one parabolic high brightness frequency band around 70 Hz. Due to the rotation speed-independent characteristic, the vibration frequency of 45 Hz is identified to be the low-order modal vibration frequency of the test bench, and the parabolic frequency band around 70 Hz may correspond to the modal frequency of the rotating shaft at the rotation speed of 4500 rpm, as the gyroscopic effect will affect the inherent frequency of the shaft when the rotation speed increases [17]. As for the frequency band of

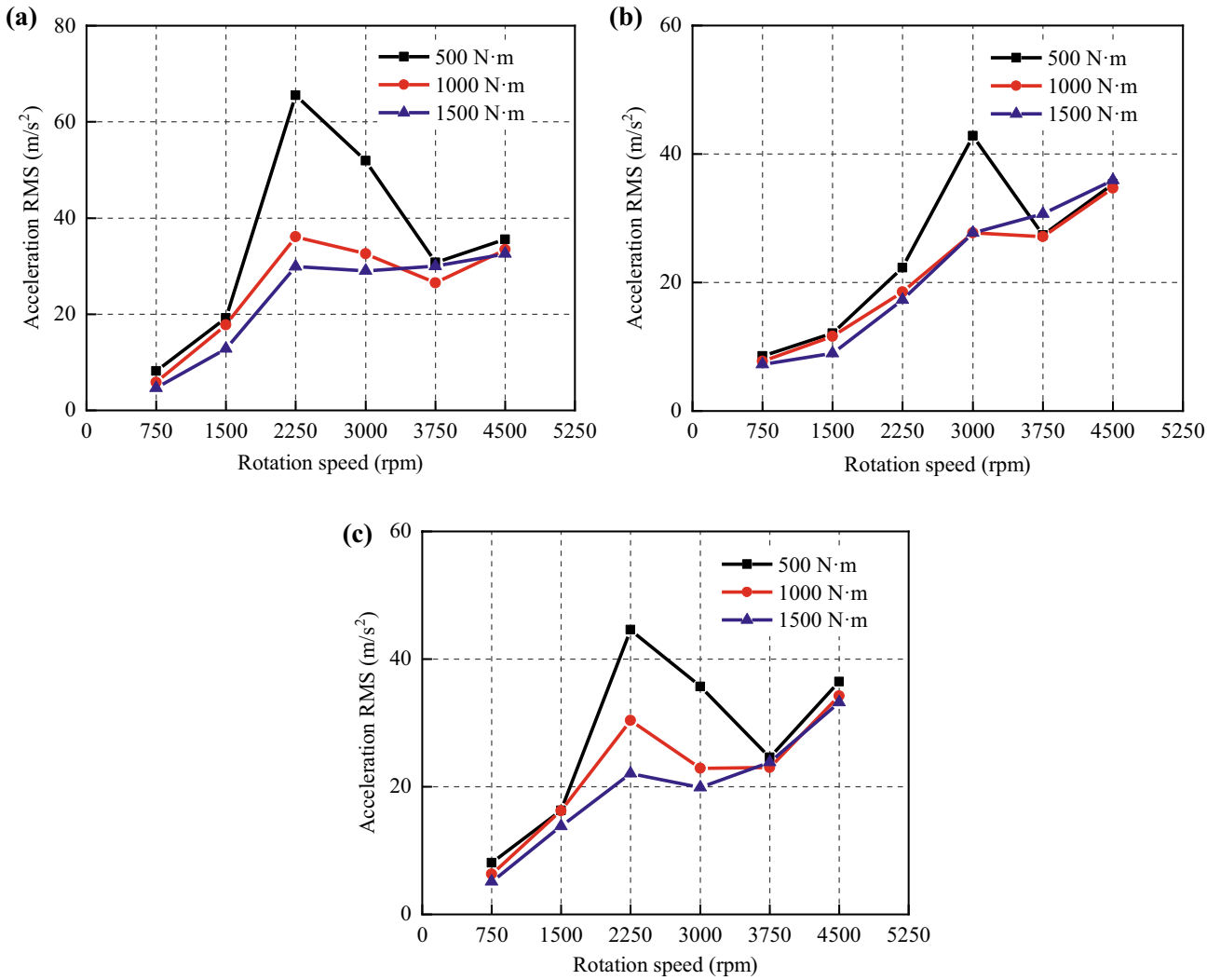

Fig. 6 Averaged RMS of the bearing bench in three directions: **a** direction *X*; **b** direction *Y*; **c** direction *Z*

500 Hz–1 kHz, the frequency of 575 Hz is identified to be the 20th-order polygonal excitation frequency of the wheel at the vehicle speed of 300 km/h [7], which has a great effect on the vibration behavior of the transmission system in all three directions.

4 Modal characteristic of the gearbox under different torques

In Sect. 3, the source of the vibration frequency around 587 Hz and 785 Hz in Fig. 10a is unknown. It is reasonable to guess that the above two frequencies should be the modal frequencies of the gearbox, which can be known from the gearbox finite element model (FEM) analysis shown in Fig. 11. The constraint condition of the gearbox in FEM analysis is illustrated in Fig. 11a. The nodes on two inner ring surfaces of the output shaft bearing bench where the gearbox bearing is installed are coupled with two "reference points" in the center, which are constrained in three translation DOFs (*X*, *Y*, *Z*) and two rotation DOFs (R_X, R_Y). Meanwhile, the two surfaces where the stacked rubber of the C-shaped bracket sits are also coupled with the two "reference points" in the center, and the vertical translation DOF (*Y*) of them is constrained, as the stacked rubber of the C-shaped bracket only provides the vertical constraint to the gearbox. It can be seen that the first two constrained modal frequencies of the gearbox FEM are respectively 527 Hz and 849 Hz, which have quite large differences with those two potential modal frequencies (587 Hz, 785 Hz) in Fig. 10a. The reason for this should be attributed to the ignorance of the gearbox bearing and gear meshing, as their stiffness characteristics have non-negligible effects on the modal frequency of the gearbox. Meanwhile, the torque will affect both the gear mesh stiffness and the bearing stiffness, and affect the modal characteristics of the gearbox consequently

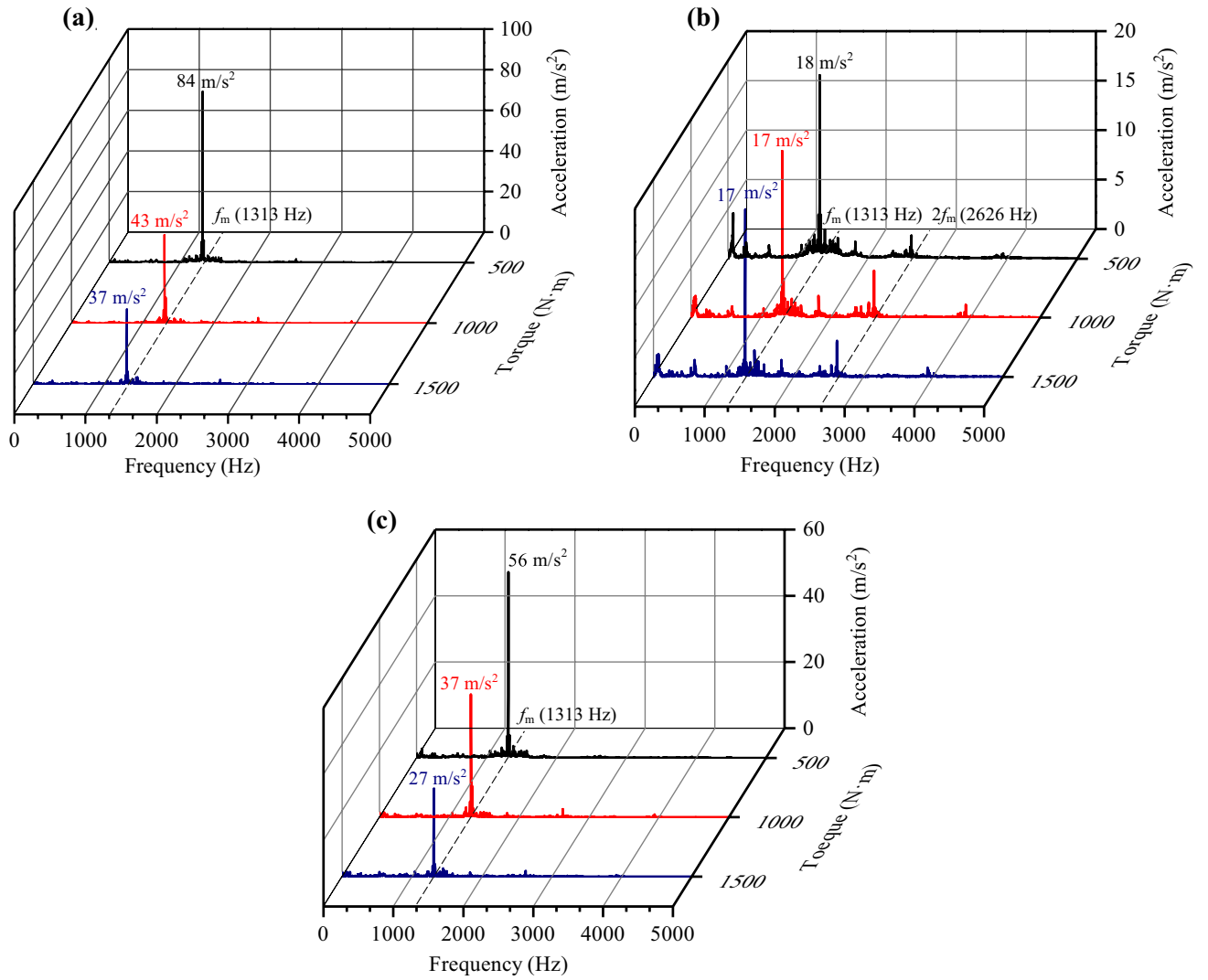

Fig. 7 Average acceleration–frequency spectrum of the bearing bench at 2250 rpm under different input torques in three directions: **a** direction *X*; **b** direction *Y*; **c** direction Z

[3, 5]. Thus, it is necessary to study the modal characteristics of the transmission system under different torques. In this section, the modal parameter of the gearbox is first identified through modal testing in Subsect. 4.1, and the sweep frequency response of the gearbox under different torques is then analyzed through dynamic modeling in Subsect. 4.2 to reveal the effect of gear meshing stiffness and bearing stiffness on the modal characteristics of the transmission system.

4.1 Modal parameter identification

The gearbox structure can be seen as a linear time-invariant (LTI) multi-input multi-output (MIMO) sub-system when the input torque is fixed, and its modal parameter can be identified from the frequency response matrix $\boldsymbol{H}_{XF}(\omega)$, in which ω represents the angular frequency, the subscripts X and F denote the response and input force, respectively. However, it is difficult to obtain the input force acting on the gearbox, which means $\boldsymbol{H}_{XF}(\omega)$ cannot be established. Fortunately, the cross-power spectrum matrix of the output response ($\boldsymbol{S}_{XX}(\omega)$) is related to $\boldsymbol{H}_{XF}(\omega)$ in the following form [15]:

$$\boldsymbol{S}_{XX}(\omega) = \boldsymbol{H}_{XF}(\omega)\boldsymbol{S}_{FF}(\omega)\boldsymbol{H}_{XF}^{\mathrm{H}}(\omega), \tag{2}$$

where superscript 'H' represent the Hermitian transpose and $\boldsymbol{S}_{FF}(\omega)$ denotes the cross-power spectrum matrix of the input force. If all input forces are white noise excitations, $\boldsymbol{S}_{FF}(\omega)$ is a frequency-independent constant matrix and $\boldsymbol{S}_{XX}(\omega)$ purely contains the modal information of the system. In order to create the required condition mentioned above, the Gaussian white noise excitation is generated in the frequency range of

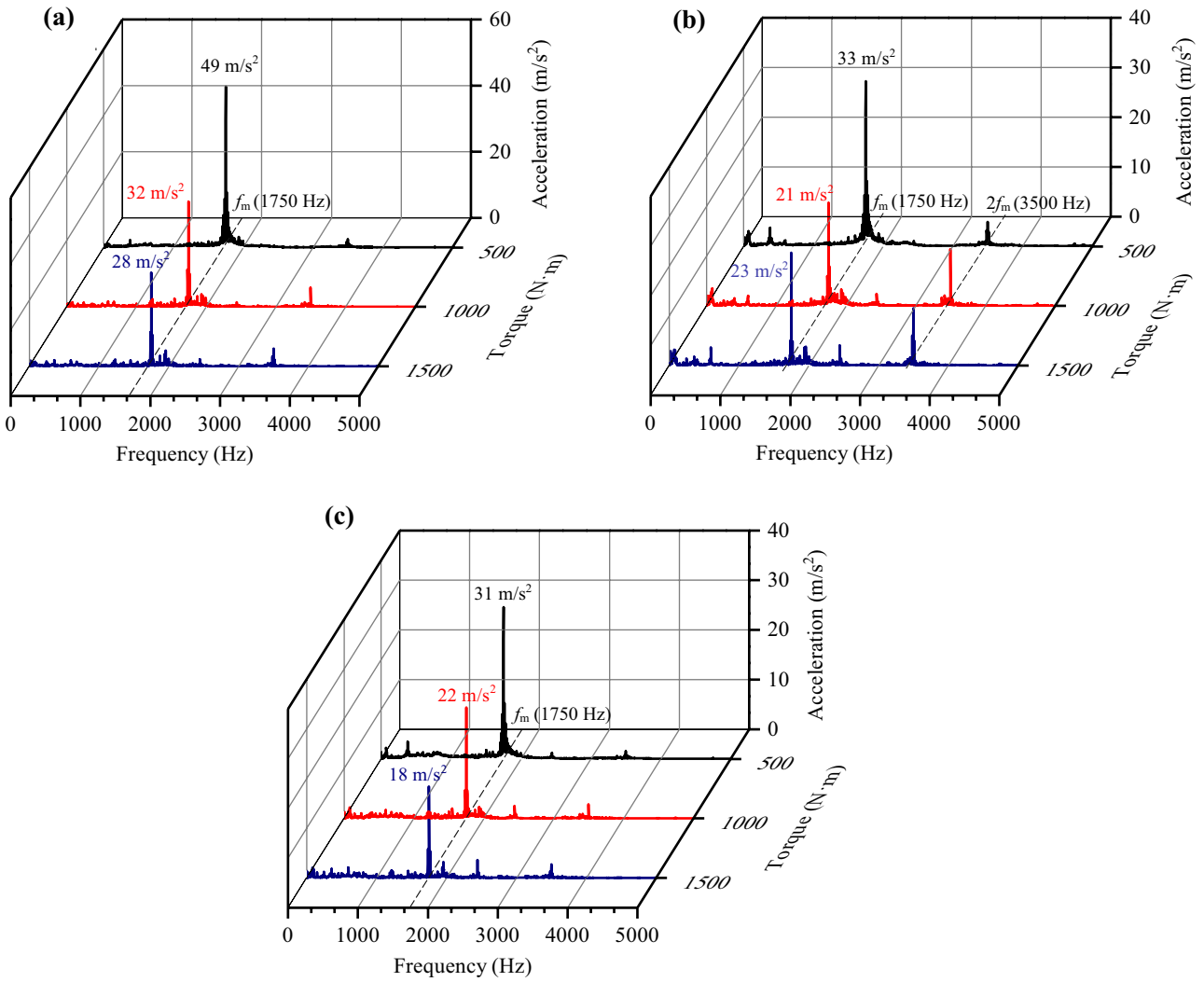

Fig. 8 Average acceleration–frequency spectrum of the bearing bench at 3000 rpm under different input torques in three directions. **a** direction *X*; **b** direction *Y*; **c** direction *Z*

500 Hz–1 kHz and used as the input signal of the actuator in the test bench. The modal parameter identification process consists of three steps: Firstly, the cross-power spectrum matrix $\boldsymbol{S}_{XX}(\omega)$ of all acceleration responses on the gearbox is estimated by Blackman–Tukey's spectral analysis method [19], and the single reference column with the maximum average power in the matrix $\boldsymbol{S}_{XX}(\omega)$ is used for modal identification. Secondly, a continuous-time state-space estimation method is performed on $\boldsymbol{S}_{XX}(\omega)$ to establish the state-space model [20]:

$$\begin{cases} \dot{\boldsymbol{x}}(t) = \boldsymbol{A}\boldsymbol{x}(t) + \boldsymbol{B}\boldsymbol{u}(t) + \boldsymbol{E}\boldsymbol{e}(t) \\ \boldsymbol{y}(t) = \boldsymbol{C}\boldsymbol{x}(t) + \boldsymbol{D}\boldsymbol{u}(t) + \boldsymbol{e}(t) \end{cases}, \tag{3}$$

where $\boldsymbol{A}$, $\boldsymbol{B}$, $\boldsymbol{C}$, $\boldsymbol{D}$, and $\boldsymbol{E}$ are the state-space matrices; $\boldsymbol{x}(t)$, $\boldsymbol{y}(t)$, $\boldsymbol{u}(t)$, and $\boldsymbol{e}(t)$ represent state, output, input, and disturbance vectors, respectively. $\boldsymbol{S}_{XX}(\omega)$ is then reconstructed from the state-space model to reduce the noise level in the original spectrum. Thirdly, the least-square rational function (LSRF) [21] estimation method is used to identify the modal parameter from the reconstructed $\boldsymbol{S}_{XX}(\omega)$, based on which, the modal vibration pattern is calculated from the state-space model identified in the second step.

Figure 12a illustrates the averaged acceleration spectrum of all elements in $\boldsymbol{S}_{XX}(\omega)$ under three input torques. It can be seen that the resonance frequency is located in the frequency range of 500 Hz–2 kHz, which is beyond the white noise excitation frequency range (500 Hz–1 kHz). Three significant peaks exist in the spectrum, which are labeled as 1st, 2nd, and 3rd, respectively. The amplitude of these peaks differs a lot under three input torques, especially for 500 N·m. It can be seen that the 3rd peak under 500 N·m is much more dominant than the other input torques, but it disappears when the input torque increases to 1000 and

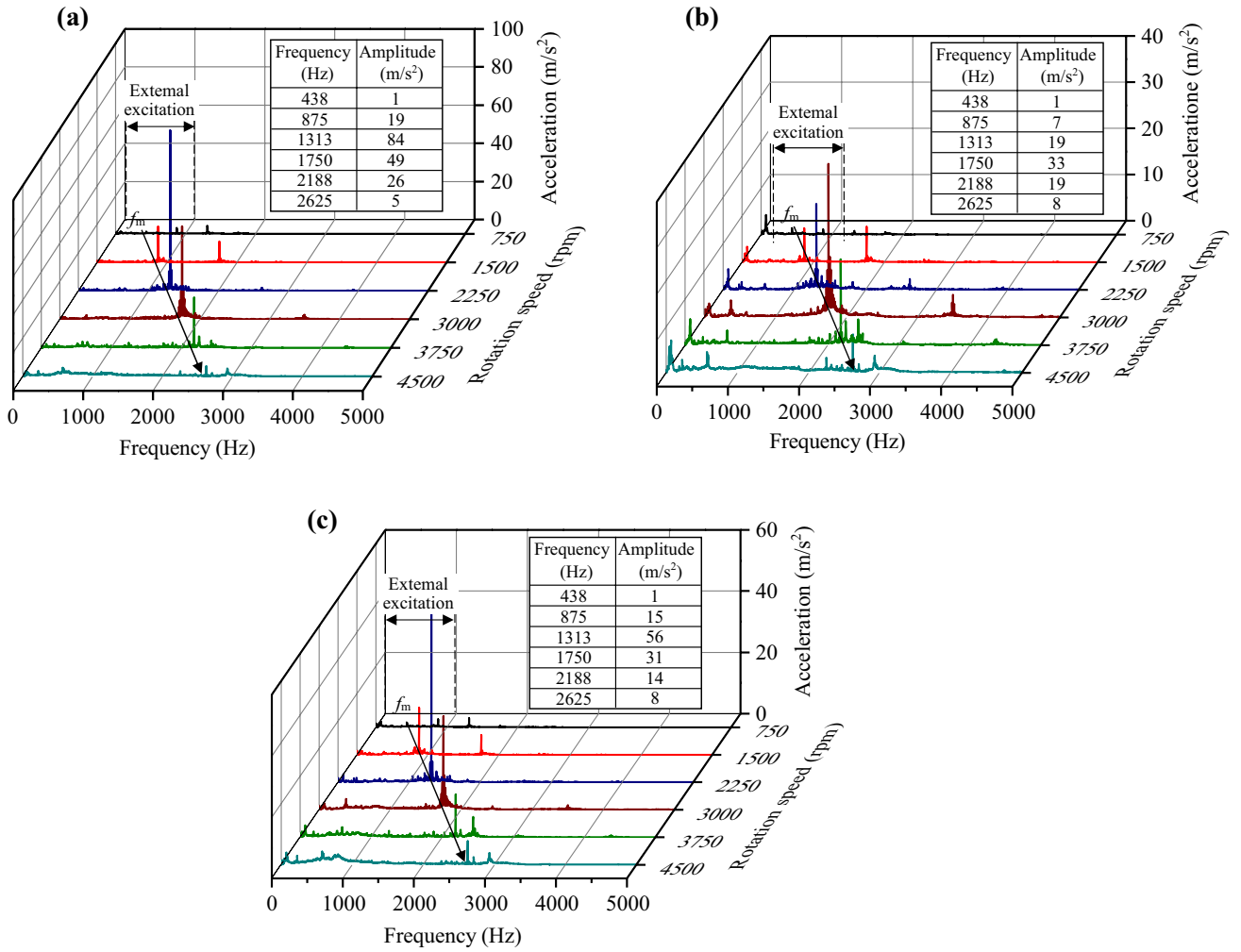

Fig. 9 Average acceleration–frequency spectrum of the bearing bench at different rotation speeds under the input torque of 500 N·m in three directions: **a** direction *X*; **b** direction *Y*; **c** direction *Z*

1500 N·m. Conversely, the 2nd peak becomes more and more dominant with the increased input torque.

Selecting the modal identification case under 500 N·m to illustrate, the modal pole is identified in the frequency range of 500 Hz–2 kHz through the stabilization diagram as shown in Fig. 12b. The continuous sequence of the cross symbol + in the stabilization diagram means the pole is stable in both modal frequency and damping ratio under the increased model order, and the stable pole with a relatively small model order in that sequence will be selected as the modal pole, which are labeled as $\sqrt{}$ in the stabilization diagram. It can be seen that except for the pole around those three significant peaks in Fig. 12a. Other stable poles located at small peaks in the spectrum are also identified.

The identified modal vibration patterns of those three significant peaks are shown in Fig. 13, in which the dashed line and solid line represent the undeformed and maximum deformed frames of the modal vibration pattern, respectively. It can be seen that the identified modal vibration pattern corresponds to the gearbox FEM modal vibration pattern in Fig. 11, which are respectively the input side vibration in direction *Z*, the output side torsion around *X*-axis, and the output side torsion around *Z*-axis.

The identification process is conducted under all three input torques, and the identified modal frequency (f_{mode}) and damping ratio (ζ_{mode}) are listed in Table 2, in which the modal index of those three significant peaks in Fig. 12a are also marked. It can be seen that the frequency of the first three modes vary in the range of 10 Hz and the damping ratio vary in the range of 0.015, which should be attributed to the noise in the original cross-power spectrum matrix and the bias in establishing the state-space model. It should be noticed that the first and third modal frequencies under 500 N·m equals 586 and 784 Hz respectively, which exactly correspond to the two unknown vibration frequencies in the average acceleration–frequency spectrum of the bearing

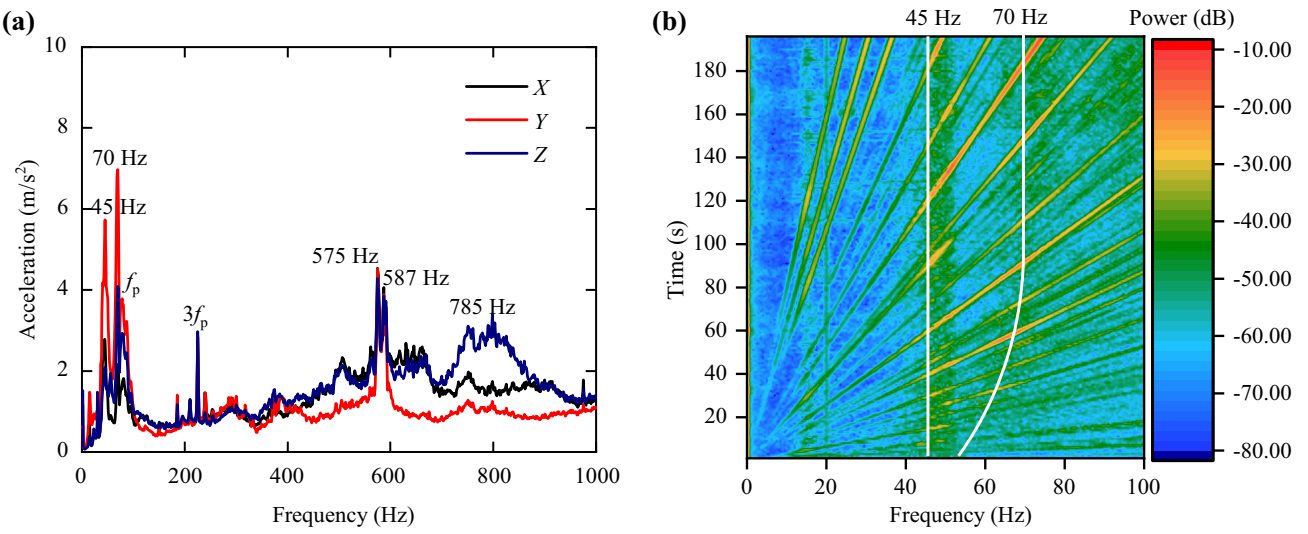

Fig. 10 **a** Zoomed-in average acceleration–frequency spectrum of the bearing bench at 4500 rpm under 500 N·m in three directions; **b** average acceleration–time–frequency spectrum during accelerating state under 500 N·m in direction *Y*

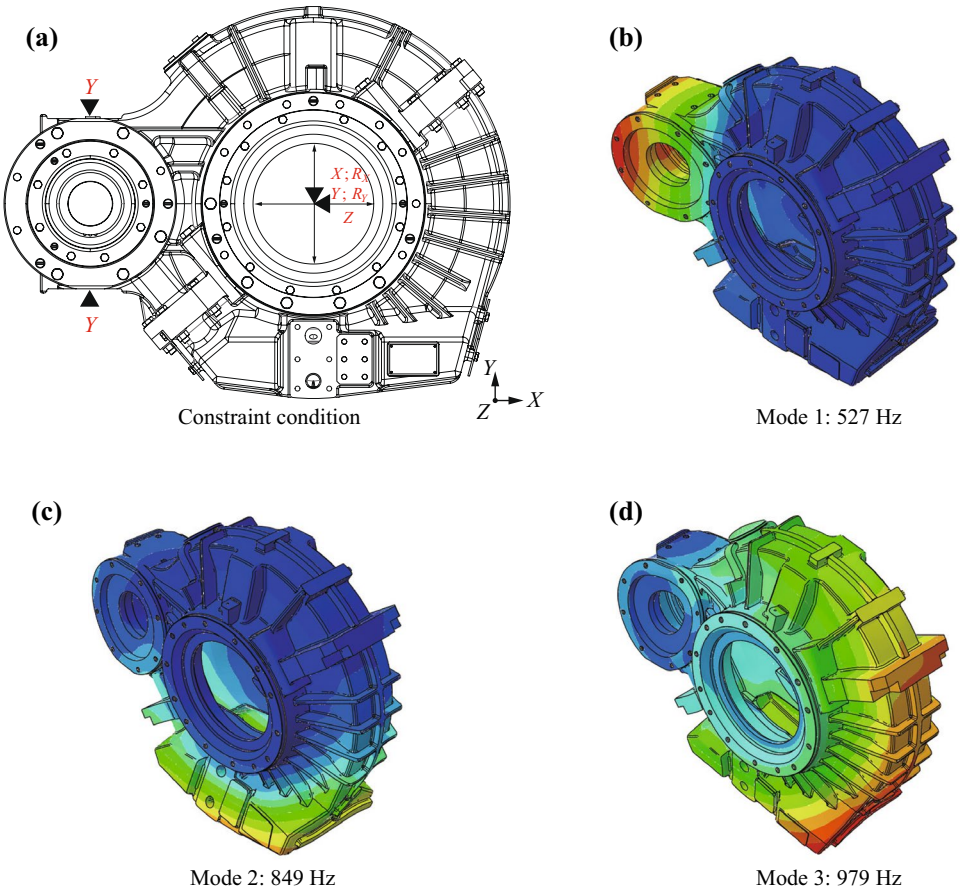

Fig. 11 Modal vibration patterns of the gearbox finite element model: **a** constraint condition; **b** mode 1; **c** mode 2; **d** mode 3

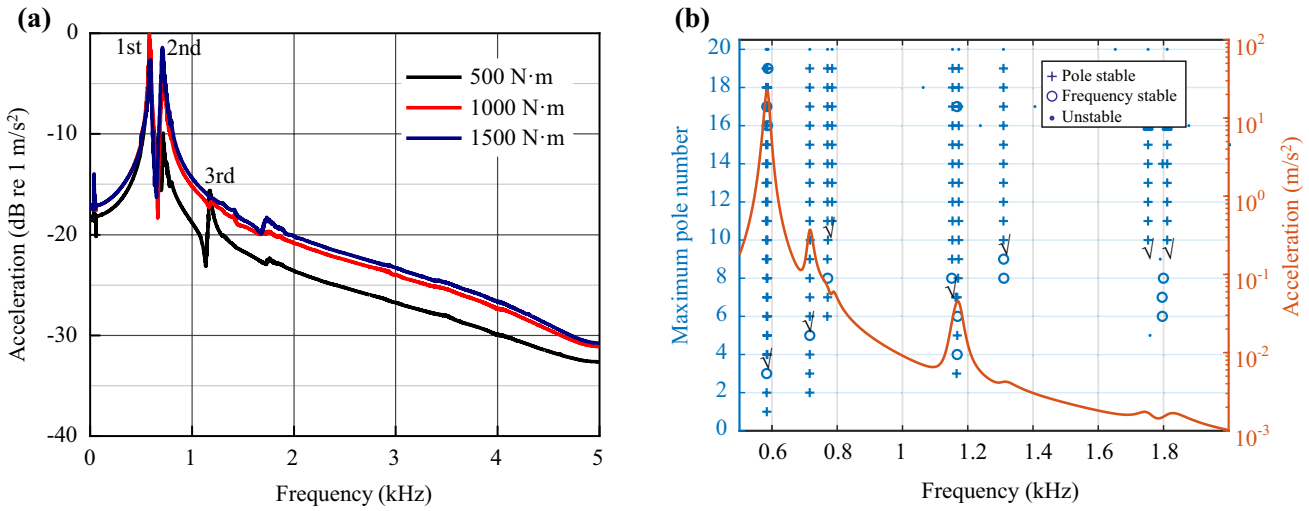

Fig. 12 **a** Averaged acceleration spectrum of all elements in $S_{XX}(\omega)$ under different torques; **b** stabilization diagram of modal identification under 500 N·m

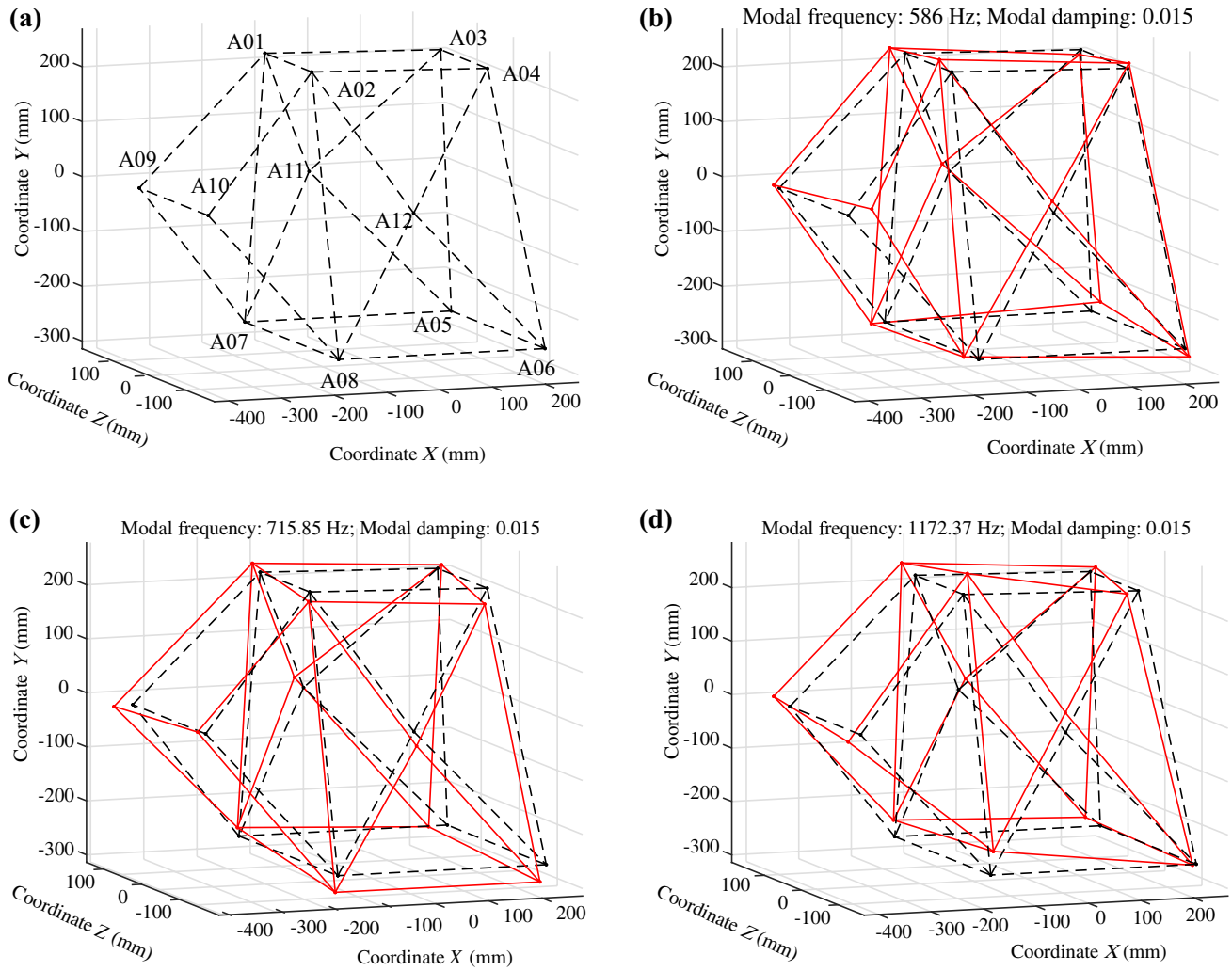

Fig. 13 Modal vibration patterns of significant peaks under 500 N·m: **a** undeformed; **b** 1st peak; **c** 2nd peak; **d** 3rd peak

Table 2 Modal parameters under three input torques

Mode No.	Modal frequency f_{mode} (Hz)			Modal damping ratio ζ_{mode}		
	500 N·m	1000 N·m	1500 N·m	500 N·m	1000 N·m	1500 N·m
1 (1st Peak)	586.00	582.71	587.69	0.015	0.012	0.024
2 (2nd Peak)	715.85	717.46	709.26	0.015	0.018	0.022
3	784.36	795.51	791.31	0.011	0.016	0.026
4 (3rd Peak)	1172.37	1174.13	–	0.015	0.017	–
5	1309.46	–	–	0.022	–	–
6	–	1432.20	1429.81	–	0.015	0.016
7	1175.57	1740.71	1720.27	0.019	0.028	0.022
8	1811.20	1864.52	1872.10	0.026	0.019	0.017

The symbol '–' means the unidentified modes

bench shown in Fig. 10a. It means the 20th-order polygonal excitation of the wheel will excite the first and third modal vibrations of the gearbox under the rated operating condition.

Meanwhile, the effect of torque is significant in identifying the fourth modal to the sixth modal. It can be seen that the fourth and sixth modes are not identified under 1500 and 500 N·m, respectively, but the fifth mode is only identified under 500 N·m. The identification result for the fifth mode should be able to explain the decreased vibration amplitude of gear meshing frequency under increased input torque in Fig. 7, as the gear meshing frequency (1313 Hz) is just located around the fifth modal frequency (1309 Hz) at the rotation speed of 2250 rpm under 500 N·m, which means that the modal resonance is excited by the gear meshing frequency. When the torque increases, the fifth mode around the gear meshing frequency no longer exists and the modal resonance disappears consequently. As for the last two modal frequencies, they show opposite trends (decreasing and increasing) with the input torque. Similarly, the decreased frequency of the seventh mode can also explain the decreased amplitude of gear meshing frequency at 3000 rpm in Fig. 8, as the seventh modal resonance (1752 Hz) is only excited by the gear meshing frequency (1750 Hz) under 500 N·m.

The fifth and seventh modal vibration patterns can also explain the different vibration behavior of the gearbox in different directions. Figure 14 illustrates the vibration pattern of the fifth mode and the seventh mode under 500 N·m. It can be seen from the fifth modal vibration pattern that the vibration of the input side on the gearbox is mainly in the directions of X and Z and that in the direction of Y is not obvious. It just explains the different vibration behavior in different directions at 2250 rpm under 500 N·m. When it comes to the seventh mode, the vibration of the gearbox input side is mainly in directions X

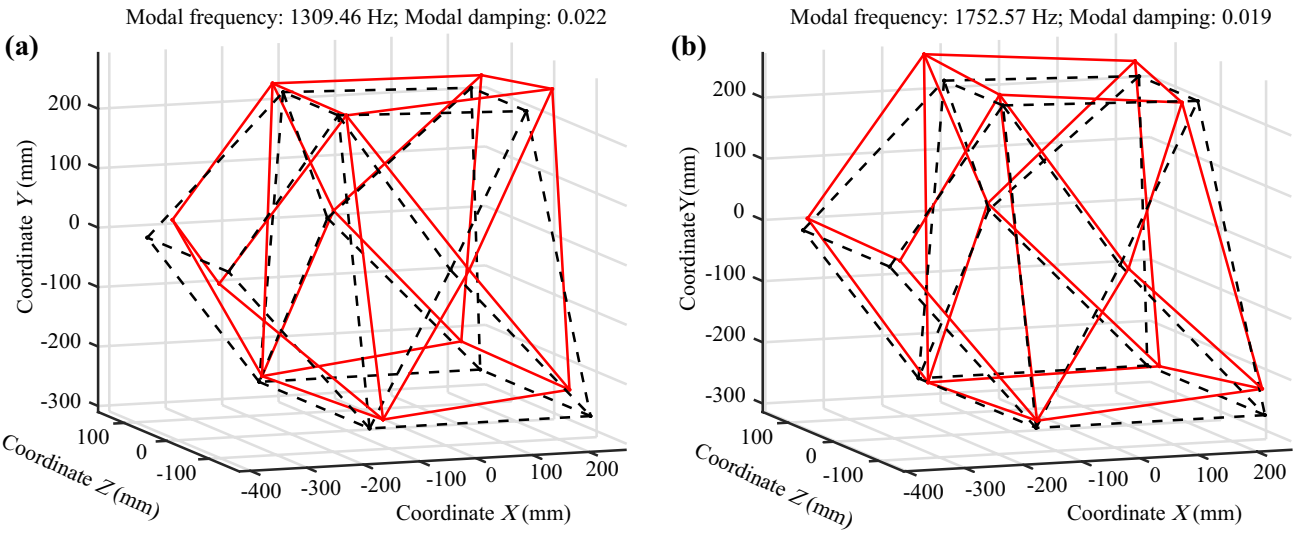

Fig. 14 Fifth and seventh modal vibration patterns under 500 N·m: **a** the fifth mode; **b** the seventh mode

and Y and the torsional vibration of the gearbox output side will be projected onto direction Z, which means that the vibrations in three directions (X, Y, Z) are obvious at 3000 rpm under 500 N·m.

4.2 Sweep frequency response analysis

The coupling relationship between the input shaft, gearbox, and output shaft is illustrated in Fig. 15. The input shaft is installed on the gearbox through two cylindrical roller bearings (NU214 and NU215) and one ball bearing (QJ214). It should be noticed that the radical constraint (X and Y) of the input shaft is provided by the cylindrical roller bearing but the axial constraint (Z) by the ball bearing only. Thus, the axial stiffness term of QJ214 is added to the stiffness matrix of NU214 when considering the coupling relationship between the input shaft and the gearbox. Meanwhile, the gearbox is installed on the output shaft through two single-row tapered roller bearings (R200W and R200M) in a face-to-face manner, the suffixes W and M stand for the wheel side and motor side of the gearbox, respectively. The input shaft and the output shaft are coupled with each other through the helical gear pair.

The way of calculating the sweep frequency response of the gearbox can be divided into four steps: Firstly, Guyan's DOF reduction theory is adopted to generate the substructure matrix of the shaft and the gearbox, as shown in Fig. 16, which are then assembled into the system matrix in a diagonal manner. It can be seen that the position of those main nodes on the gearbox exactly corresponds to the tested acceleration sensors in Fig. 5 and that on shaft contains all coupling points with gear pair and bearings. The total DOF number of the system is 77, which is sufficient to catch the mode with the frequency

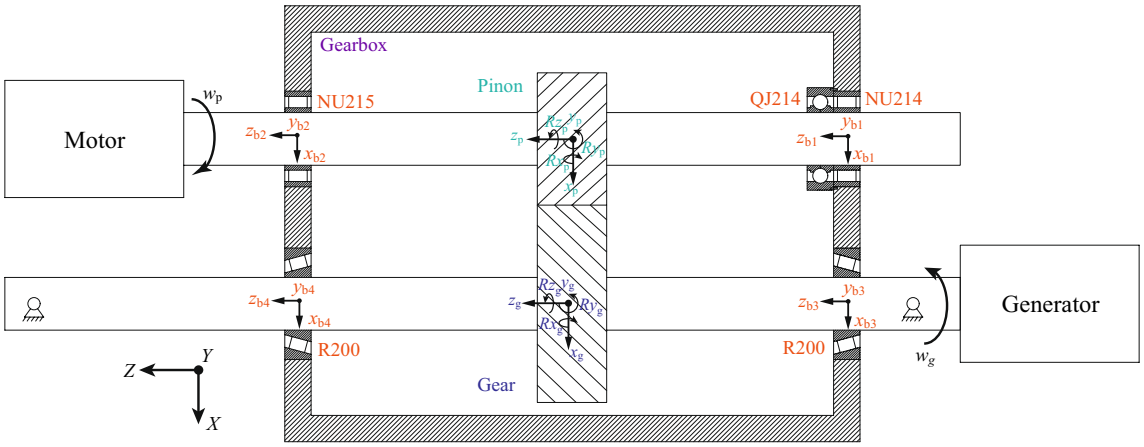

Fig. 15 Configuration of the transmission system

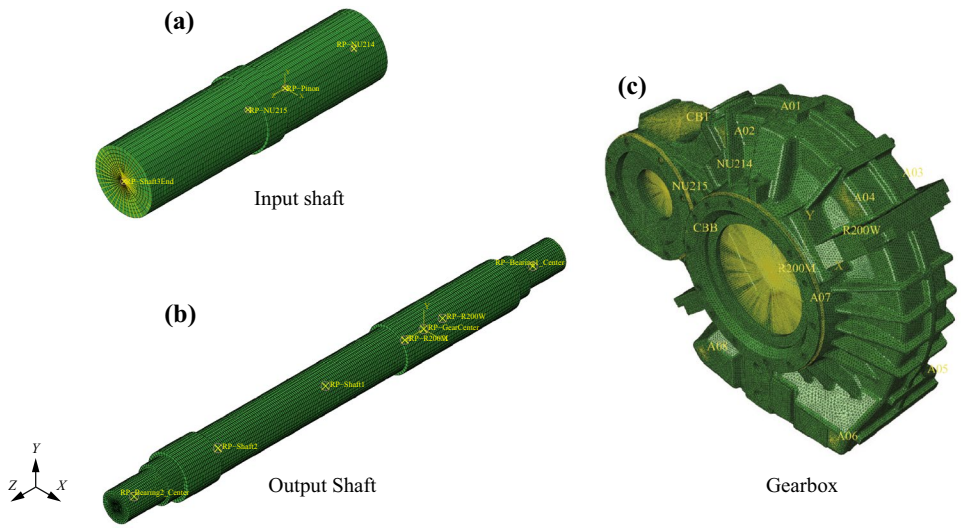

Fig. 16 Selection of main nodes in generating input shaft, output shaft, and gearbox substructures

below the maximum gear meshing frequency in the bench test. Secondly, the method developed by Chang et al. [5] is adopted to calculate the time-varying gear meshing stiffness (TVMS) under different torques. The averaged value of TVMS is used in establishing the coupling stiffness matrix between the gear pair, and the amplitude of the variation term of TVMS is used as the gear meshing excitation force. Thirdly, the bearing stiffness matrix is to be calculated under different torques in a quasi-static manner. Given each torque condition, the total load on each bearing in the system can be calculated by static analysis, which is then used to calculate the time-varying stiffness of each bearing by solving the equilibrium iteratively. The averaged value of the bearing stiffness matrix is then used as the coupling term in the system stiffness matrix. Finally, the sweep frequency acceleration response of the gearbox ($\boldsymbol{G}(\omega_m)$) can be derived through the following equation:

$$\boldsymbol{G}(\omega_m) = (j\omega_m)^2\left(\boldsymbol{K} - \omega_m^2\boldsymbol{M}\right)^{-1}\boldsymbol{F}_m, \tag{4}$$

where $\boldsymbol{K}$ and $\boldsymbol{M}$ are the assembled stiffness matrix and mass matrix of the transmission system, respectively; ω_m and $\boldsymbol{F}_m$ represent the gear meshing angular frequency ($\omega_m = 2\pi f_m$) and the unit vector of the gear meshing force, respectively; j is the imaginary unit.

The averaged gear meshing stiffness as well as the main diagonal element in the bearing stiffness matrix are listed in Table 3. It can be seen that the torque has positive correlations with both the gear meshing stiffness and bearing stiffness, which will lead to the variation of the modal resonance peak in the averaged sweep frequency response curve of the gearbox, as shown in Fig. 17a. Figure 17b illustrates the averaged sweep frequency response curve under 500 N·m, in which the gear meshing frequencies that the tested speed conditions corresponded to are marked as the dashed line. It can be seen that the amplitude of the intersection points between the sweep frequency response and the dashed line share the same variation behavior with the RMS value in Fig. 6.

In summary, the torque has a great effect on the modal characteristic of the gearbox, which is the inherent reason for the different vibration behavior observed in Fig. 6. Meanwhile, the gear meshing frequency can excite the modal vibration of the gearbox at both the rotation speeds of 2250 and 3000 rpm under the input torque of 500 N·m, which should be avoided in the real operational scenario.

Table 3 Averaged stiffness of gear meshing and bearing

Name	Averaged stiffness (kN/mm)		
	500 N·m	1000 N·m	1500 N·m
Gear meshing	909.28	1108.22	1242.83
NU214-X	829.49	926.39	1001.35
NU214-Y	452.04	605.68	706.29
NU214-Z	218.85	279.86	324.86
NU215-X	642.95	740.98	846.16
NU215-Y	941.71	1133.82	1216.26
R200W-X	760.11	967.1	1098.71
R200W-Y	38.50	115.39	170.33
R200W-Z	94.68	128.34	150.46
R200M-X	7252.05	7763.61	8083.67
R200M-Y	7256.64	7817.39	8149.95
R200M-Z	1720.17	1847.31	1924.68

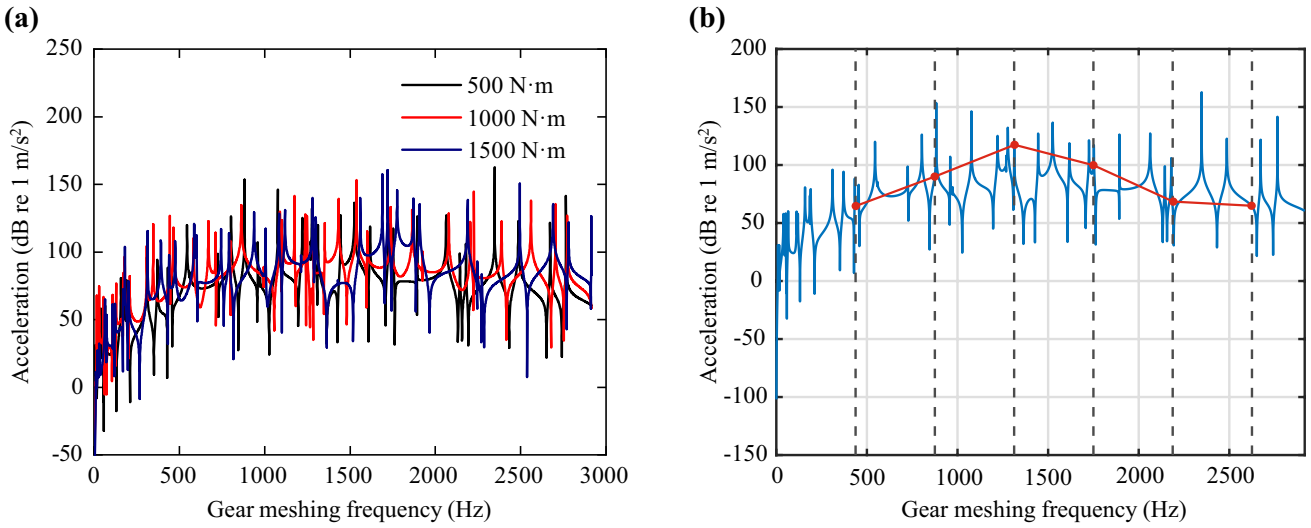

Fig. 17 Averaged sweep frequency response curve of the gearbox under gear meshing excitation: **a** 500–1500 N·m; **b** 500 N·m

5 Conclusion

Based on the high-speed train transmission system test bench, the excitation condition covering both internal and external is created. The vibration behavior and the modal characteristic of the high-speed train gearbox are studied under various operating conditions. Main conclusions are obtained as follows:

- The vibration behavior of the gearbox is strongly related to both the torque and rotation speed. When the input torque is fixed at 500 N·m, the vibration of the gearbox will suffer severe vibration at the rotation speeds of 2250 and 3000 rpm, and the increased torque will attenuate the vibration intensity at the above two rotation speeds.
- The gear meshing frequency and its harmonics dominate the gearbox vibration at most of the rotation speeds (750–3750 rpm). However, when the input shaft is rotating at 4500 rpm, the external excitation will affect the gearbox vibration significantly in the frequency band of 0-1 kHz, and excite the modal vibration of the transmission system.
- The torque affects both the modal frequency and the modal vibration pattern of the gearbox, which is also the reason for the attenuation effect of the increased torque on the gearbox vibration intensity at the rotation speeds of 2250 and 3000 rpm. The gear meshing frequency at the above two rotation speeds will excite the fifth and seventh gearbox modal vibration under the input torque of 500 N·m.
- When the torque increases from 500 to 1500 N·m, the fifth and seventh modal frequencies shift away and the modal resonance is no longer excited. The variation of gear meshing stiffness and bearing stiffness under different torques is the inherent reason for the shift of modal frequency, which will affect the vibration behavior of the gearbox significantly.

Acknowledgements The authors are grateful for the financial support from the National Key Research and Development Program of China (Grant No. 2021YFB3400701) and the Fundamental Research Funds for the Central Universities (Science and technology leading talent team project, Grant No. 2022JBQY007).

References

1. Kahraman A, Singh R (1990) Non-linear dynamics of a spur gear pair. J Sound Vib 142(1):49–75
2. Kahraman A, Singh R (1991) Interactions between time-varying mesh stiffness and clearance non-linearities in a geared system. J Sound Vib 146(1):135–156
3. Fernandez-del-Rincon A, Garcia P, Diez-Ibarbia A et al (2017) Enhanced model of gear transmission dynamics for condition monitoring applications: effects of torque, friction and bearing clearance. Mech Syst Signal Process 85:445–467
4. Fernández A, Iglesias M, de-Juan A, et al (2014) Gear transmission dynamic: effects of tooth profile deviations and support flexibility. Appl Acoust 77:138–149
5. Chang L, Cao X, He Z et al (2018) Load-related dynamic behaviors of a helical gear pair with tooth flank errors. J Mech Sci Technol 32(4):1473–1487
6. Wang Z, Cheng Y, Mei G et al (2020) Torsional vibration analysis of the gear transmission system of high-speed trains with wheel defects. Proc Inst Mech Eng Part F J Rail Rapid Transit 234(2):123–133
7. Wang Z, Mei G, Zhang W et al (2018) Effects of polygonal wear of wheels on the dynamic performance of the gearbox housing of a high-speed train. Proc Inst Mech Eng Part F J Rail Rapid Transit 232(6):1852–1863
8. Hu W, Liu Z, Liu D et al (2017) Fatigue failure analysis of high-speed train gearbox housings. Eng Fail Anal 73:57–71
9. Zhang B, Tan ACC, Lin JH (2016) Gearbox fault diagnosis of high-speed railway train. Eng Fail Anal 66:407–420
10. Huang GH, Zhou N, Zhang WH (2016) Effect of internal dynamic excitation of the traction system on the dynamic behavior of a high-speed train. Proc Inst Mech Eng Part F J Rail Rapid Transit 230(8):1899–1907
11. Huang GH, Xu SS, Zhang WH et al (2017) Super-harmonic resonance of gear transmission system under stick-slip vibration in high-speed train. J Cent South Univ 24(3):726–735
12. Wei J, Zhang A, Wang G et al (2018) A study of nonlinear excitation modeling of helical gears with modification: theoretical analysis and experiments. Mech Mach Theory 128:314–335
13. Lu X, Chen H, He X (2022) Operational modal parameter identification with correlated colored noise excitation. J Vib Contr 28(17–18):2435–2444
14. Li X, Antoni J, Brennan MJ et al (2020) A frequency domain blind identification method for operational modal analysis using a limited number of sensors. J Vib Contr 26(17–18):1383–1398
15. Kocan C (2020) A comparative study on in-flight modal identification of an aircraft using time- and frequency-domain techniques. J Vib Contr 26(21–22):1920–1934
16. Zhang T (2018) Modal identification of gearbox housing of high speed train under assembly condition. J Mech Eng 54(12):31
17. Stringer DB (2008) Gear modeling methodologies for advancing prognostic capabilities in rotary-wing transmission systems. Dissertation, University of Virginia.
18. Hayes MH (1996) Statistical digital signal processing and modeling. John Wiley, New Jersey
19. Ljung L (1999) System identification: theory for the user, 2nd edn. Prentice Hall, New Jersey
20. McKelvey T, Akçay H, Ljung L (1996) Subspace-based multivariable system iden- tification from frequency response data. IEEE Trans Automat Contr 41(7):960–979
21. Arda Ozdemir A, Gumussoy S (2017) Transfer function estimation in system identification toolbox via vector fitting. IFAC-PapersOnLine 50(1):6232–6237